

# Investigation Of Structural, Ferroelectric, Impedance And Conduction Mechanism In $\text{Gd}^{3+}$ Modified $\text{PbTiO}_3$ Ferroelectric Perovskites

Jagvir Singh<sup>1</sup>, Dr. Sunil Kumar Dwivedi<sup>2</sup>, Dr. Sandeep Sharma<sup>3</sup>

<sup>1</sup>Research Scholar, Department of Physics, Om Sterling Global University, Hisar

<sup>2</sup>Associate Professor, Department of Physics, Om Sterling Global University, Hisar

<sup>3</sup>Associate Professor, HOD Department of Physics, S. R. R. M. Govt College, Jhunjhunu, Rajasthan

Email id: [jagvirphy221@osgu.ac.in](mailto:jagvirphy221@osgu.ac.in)<sup>1</sup>; [ksunildwivedi@gmail.com](mailto:ksunildwivedi@gmail.com)<sup>2</sup>; [sharma.jjn39@gmail.com](mailto:sharma.jjn39@gmail.com)<sup>3</sup>

Trivalent metal ion ( $\text{Gd}^{3+}$ )modified  $\text{PbTiO}_3$  ( $\text{Pb}_{1-x}\text{Gd}_x\text{TiO}_3$ ,  $x = 0.22$  &  $0.25$ ) ferroelectric perovskites have been synthesized using solid solutions. Structural analysis from x-ray diffraction reveals that prepared solid solution crystallizes in tetragonal phase whereas S-shaped Polarization vs. Applied Electric Field confirms presence of ferroelectric polarization. Maxima in  $\epsilon'$  vs. Temperature profile represents ferroelectric to paraelectric transition whereas lower  $T_c^{\text{FE}}$  corresponds to reduction in tetragonality due to partial substitution of  $\text{Gd}^{3+}$  at  $\text{Pb}^{2+}$ . This modification also leads towards decrease in cell volume as well as non centrosymmetry in prepared ferroelectric perovskites. Prepared ferroelectric solid solutions has also been characterized for temperature dependent dielectric, impedance and conductivity response and influence of hetrovalancy substitution as well as temperature on electric modulus, dielectric relaxation, resistive and conductive behavior in from 100 Hz to 1 MHz frequency regime reported. The hopping mechanism resulted due to thermally activated dipoles stamped for tailoring dielectric, conductive and impedance response. The effect of hetrovalancy substitution leads in creation of oxygen vacancies responsible for improvement in conductivity has been analyzed and reported. The maxima in imaginary part of electrical modulus evident for appearance of relaxation phenomenon. The shift in maxima in  $\tan \delta$  vs. Temperature at different frequency responsible for presence of frequency as well as temperature dependent dielectric relaxation in ( $\text{Gd}^{3+}$ )modified  $\text{PbTiO}_3$ . The conductivity behavior has been analyzed using universal power law and  $n$  (Obtained from power law fitting) vs. Temperature lights up about conduction mechanism. The increase in value of dielectric constant with increasing temperature directly signature for thermally activation of dipoles whereas decrease in value of real part of impedance as well as electric modulus reveals increase in conducting response led by increase in concentration of oxygen vacancies resulted due to charge im-balance created by substitution of  $\text{Gd}^{3+}$  at  $\text{Pb}^{2+}$  in  $\text{PbTiO}_3$  ferroelectric ceramic solid solutions.

**Keywords:** Ferroelectric Perovskite, Hopping, Dielectric Relaxation, Space Charge Polarization, Remnant Polarization ( $P_r$ )

## 1. Introduction

Perovskites are a class of materials that have the general formula  $ABX_3$  where A and B are cations with very different sizes (with A is cations typically being much larger than other cation B) and X is an anion (frequently oxygen) bonded to both the cations. In general, oxide perovskites have always been known for various properties like dielectric, ferroelectric, piezoelectric, catalytic, ionic and electronic conduction results in wide range of applications. Lead titanate ( $PbTiO_3$ ), Barium titanate ( $BaTiO_3$ ), Strontium titanate ( $SrTiO_3$ ), Calcium titanate ( $CaTiO_3$ ) & Lead zirconate ( $PbTi_{1-x}Zr_xO_3$ ) are a few common and mostly studied examples of ferroelectric perovskites. Among all these perovskites, alkaline earth Titanate  $MTiO_3$  (where M is divalent ion = Ba, Sr, Ca&Pb) attracted a lot of attention due to their unique dielectric, ferroelectric and piezoelectric properties which are of immense interest in technological applications like capacitors, actuators, transducers and non-volatile random access memory devices.  $SrTiO_3$  which is one of an important n-type semiconductor with band gap of 3.2 eV has high stability and wavelength response making it a promising candidate for photo catalysis, photo electrode and water splitting applications.  $CaTiO_3$  has not been widely developed due to lack of interest in practical applications but is used as a compositional substitute in other perovskites for controlling ferroelectricity. Like ferromagnetic materials, the functional properties of ferroelectric materials find wide range of applications, ranging from actuators and sensors to memory or optical devices. So before we define the ferroelectric materials, we should classify dielectric materials. Dielectric is belonging to a class of insulating materials that on the application of an electric field shows dielectric polarization [1-6]. Here the center of symmetry plays a significant role for their properties. Crystal structure with a center of symmetry have such an arrangement of atoms around a point or center that by the inversion, we can get the same arrangement of atoms in the crystal. Dielectric materials belong to a group of non-Centro symmetric crystal structure. Among all point group, only non-Centro symmetric point group shows piezoelectric properties. The properties due to which voltage obtains from charge separation as well as mechanical stress and vice versa. Both direct and inverse piezoelectric effects have a wide range of application in electronic devices. Barium or Lead Titanate is an example of non-centrosymmetric piezoelectric material used in microphone and transducer. In non-centrosymmetric crystals there is an axis of symmetry, called polarity. The cells of polar structure have efficient dielectric polarization, so often called a spontaneous polarization. Either by stress or by a change in temperature the dipole moment of these polar [6-10].

$PbTiO_3$  is a well-known ferroelectric material which finds significant use as a component material in electronics such as capacitors, ultrasonic transducers, and optoelectronics. With the establishment of high entropy alloys, researchers have explored various multicomponent oxides. It has been already reported that substitution of rare earth ion ( $Nd^{3+}$  &  $Gd^{3+}$ ) at  $Pb^{2+}$  site in  $PbTiO_3$  results in reduction of ferroelectric transition temperature, improved conductivity, lowering ferroelectric polarization prepared by different methods (Solid state reaction route as well as Auto-Combustion method) [11-17]. The effect of sintering temperature results in increase in ferroelectric polarization whereas sample prepared using auto-combustion method exhibits lesser ferroelectric polarization as compare to sample prepared using solid state reaction route whereas ferroelectric transition temperature in all cases (sample sintered at different temperature as well as sample prepared using different synthesis method) remains same because crystal structural phase in all sample is tetragonal

phases. The sample prepared using different synthesis approaches as well as effect of sintering temperature results in two conduction mechanism followed by samples in entire temperature range. Below 500 °C, sample obeys small polaron hopping model whereas above this temperature, sample obeys carrier barrier model.

In this investigation, we are reporting functional properties of phase-pure multicomponent  $\text{Gd}^{3+}$ -modified lead titanate ( $\text{PbTiO}_3$ ) perovskite synthesized by solid state reaction route approach Influence of rare earth ( $\text{Gd}^{3+}$ ) substitution on ferroelectric transition temperature, conductivity as well as ferroelectric polarization, dielectric relaxation, impedance response has been explored and reported.

## 2. Experimental and Characterization:

Rare earth ( $\text{Gd}^{3+}$ ) modified  $\text{PbTiO}_3$  ( $\text{Pb}_{1-x}\text{Gd}_x\text{TiO}_3$ ,  $x = 0.22$  &  $0.25$ ) ferroelectric perovskites solid solutions have been synthesized using conventional high energy ball milling process. This approach has been commonly known as solid state reaction route. For this, oxide of required metal ions ( $\text{PbO}$ ,  $\text{TiO}_2$  &  $\text{Gd}_2\text{O}_3$ ) have been taken as raw materials and weighed according to mentioned stoichiometric proportionate and ball milling using high energy ball milling machine, zirconia balls, non-reacting solvent (Water, Acetone or Propanol) and platinum zar. The milling process running for 24 hours so that all metal oxides mixed together properly along with reduction in particle size. After completion of milling process, mixed powder taken out from platinum zar and left for dry. The dried powder transfers into alumina crucible and calcined for 12 hours at 1000 °C in closed crucible arrangement for structural phase formation. The calcined powder mixed with polyvinyl alcohol for making pellets for sintering process. The pellets were then sintered at 1200 °C in  $\text{PbO}$  environment in closed crucible system to encounter volatility of  $\text{Pb}^{2+}$ . The crystal structure and phase purity, morphology and particle size and elemental composition of the pellets prepared were determined from diffraction data collected using X-ray diffraction (XRD) whereas morphological as well as elemental analysis carried out scanning electron microscopy (SEM) and energy dispersive spectroscopy (EDS) respectively. Ferroelectric transition (Ferroelectric to Para electric) temperature has been confirmed studied from  $\epsilon'$  vs. Temperature profile whereas ferroelectric polarization (Polarization vs. Electric Field) hysteresis recorded using ferroelectric tester. The influence of  $\text{Gd}^{3+}$ -substitution on dielectric relaxation as well as conductivity behavior of  $\text{PbTiO}_3$  have been studied using impedance analyzer interfaced with high temperature furnace. The effect of sintering process on density of prepared solid solutions has been studied from Archimedes principle based lab made set by calculating density. Sintered Pellets have been used to study high temperature dielectric, impedance & conductivity properties using complex impedance spectroscopy. The real and imaginary components of electrical impedance as well as dielectric permittivity has been studied using complex impedance spectroscopy. Conduction mechanism from universal johncher's power fitting of conductivity data at different temperatures has been studied using complex impedance spectroscopy (CIS). This is valuable and important characterizing technique in material science. These electrical properties were ascertained using Keysight Technologies (E4990A) using impedance analyzer. All of these characteristics were calculated from empirically acquired  $Z$  versus  $\theta$  at various temperatures using recognized equations.

$$\text{Complex Impedance, } Z^* = Z' - jZ''$$

Complex dielectric constant,  $\varepsilon^* = \varepsilon' - j\varepsilon''$

Complex electric modulus,  $M^* = M' + jM''$

$$\text{Also, } \tan \delta = \frac{\varepsilon''}{\varepsilon'}$$

Where  $Z', \varepsilon', M'$  and  $Z'', \varepsilon'', M''$  denote the real and imaginary parts of the impedance, dielectric constant and electric modulus respectively and  $j = \sqrt{-1}$ . Using Jonscher's power law [11] to study conduction process

$$\sigma_{ac} = \sigma_{dc} + A\omega^n$$

"A" denotes the dispersion parameter describing the strength of Polarizability; "dc" denotes "dc conductivity," "ac" denotes "ac conductivity," and so on. "n" is a dimensionless quantity that gives information on the interaction between mobile ions and the lattice in which they interact. The information about the conduction mechanism followed by prepared samples extracted from n (Obtained from universal Jonscher's power law) vs. Temperature profile.

### 3. Results and Discussion

#### Crystal Phase Analysis

Structural phases formed in prepared  $\text{Pb}_{1-x}\text{Gd}_x\text{TiO}_3$ ,  $x = 0.22$  &  $0.25$  ferroelectric perovskite solid solutions have been investigated from x-ray diffraction data. Room temperature X-ray diffraction data of  $\text{Pb}_{1-x}\text{Gd}_x\text{TiO}_3$ ,  $x = 0.22$  &  $0.25$  has been shown in Figure 1. The crystalline behavior of the produced ceramic composite solid solutions has been revealed from high intense sharply edged high intensity diffraction peaks whereas least broadening or sharpness of peaks evident for nano-sized crystallite formed. For analysis of crystal structural phase, diffraction data ( $2\theta$  vs. Intensity (a.u.)) of prepared ferroelectric solid solutions have been studied by comparing it with similar structural phase reported or by comparing peak positions of diffraction data with diffraction data of similar compound reported in JCPDS cards to explore specific crystal structure (d-spacing, Lattice parameters, etc.). Using JCPDS cards of tetragonal phases of resembles with pure  $\text{PbTiO}_3$  & modified  $\text{PbTiO}_3$  by substitutional, all diffraction peaks were examined and indexed. The diffraction peaks listed on JCPDS card no. 78-0299 represents tetragonal structural phase (Space Group No. 99 and symbol  $P4mm$ ). Diffraction peaks particularly appears at  $2\theta \sim 22.7$  &  $31.7$  reveals presence of tetragonal phase  $\text{PbTiO}_3$ . No peak left unindexed confirms no secondary phase appears other than tetragonal phase also evidences for successful ceramic composite solid solutions

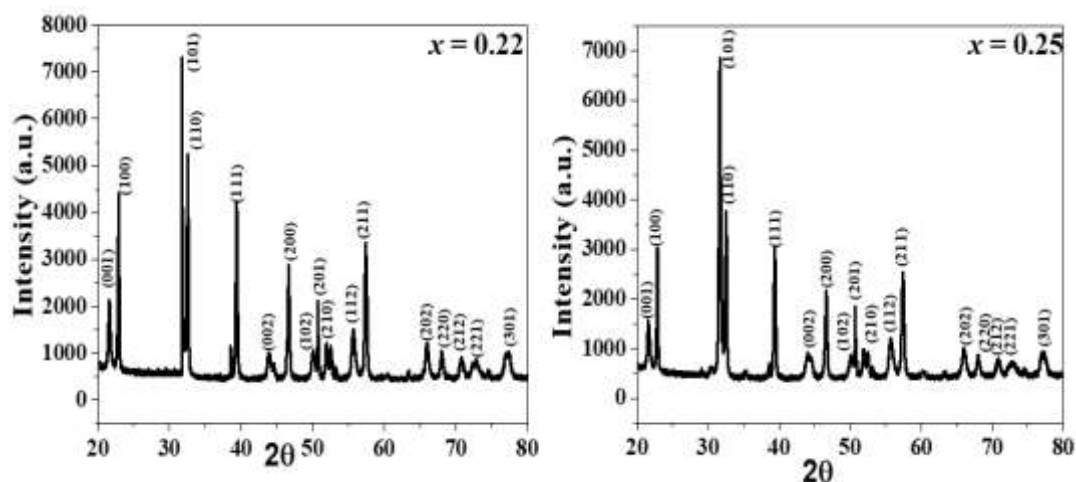


**Figure 1: X-Ray Diffraction Pattern of  $\text{Pb}_{1-x}\text{Gd}_x\text{TiO}_3$ ,  $x = 0.22$  &  $0.25$  ferroelectric perovskites solid solutions**

The lattice parameters of prepared ferroelectric perovskites have been calculated using following equation:

$$1/d_{hkl}^2 = (h^2 + k^2)/a^2 + l^2/c^2$$

Where  $h$ ,  $k$  and  $l$  are Miller indices,  $\beta$  ( $= 99.54^\circ$ ) is lattice angle and  $d$  stands for inter-planer spacing obtained from Bragg's diffraction law. The lattice parameter has been tabled in table 1 given below. This diffraction data has also used to analyze various another factor such as crystallite size, dislocation density, micro-strain, using different-different formulae given below

$$D = \frac{0.9\lambda}{\beta \cos \theta}$$

$$\varepsilon = \frac{\beta \cos \theta}{4}$$

$$\delta = \frac{1}{D^2}$$

the calculated parameters have also been table in table 1 along with lattice parameters. It has been clearly seen from table that lattice parameters slightly change with increases  $\text{Gd}^{3+}$  substitution (lattice parameter ' $a$ ' slightly decreases whereas ' $c$ ' increases) as reported in JCPDS card mentioned above to analyze structural phase and miller indices. Further diffraction pattern clearly reveals that as concentration of  $\text{Gd}^{3+}$  in stoichiometric proportion of solid solution has been increases, a considerable shift of diffraction peaks towards higher diffraction angle ( $2\theta$ ) visualized. This shift in position of diffraction peaks with composites stoichiometric proportion may results due to variation of average crystallite size (either increase or decrease) as well as of unit cell volume of tetragonal structural phase. This shift in position of diffraction peaks also indicate towards shift in atomic position as well as lattice parameters of both phase. It has been clearly visualized from table 1 that average crystallite size decreases with increasing concentration of  $\text{Gd}^{3+}$  in stoichiometric proportion of solid solution also results to lower tetragonality which also justified from decrease in ferroelectric transition temperature.

**Table 1: Crystallographic Signatures (Lattice Parameters (a & c), Crystallite Size (D),  $\varepsilon$  = Strain,  $\delta$  = Dislocation Density & c/a vs. Composition (x) of  $\text{Pb}_{1-x}\text{Gd}_x\text{TiO}_3$ , x = 0.22 & 0.25 ferroelectric perovskites solid solutions**

Composition (x)	'a=b' [Å]	'c' [Å]	D = Crystallite Size	$\varepsilon$ = Strain	$\delta$ = Dislocation Density	c/a
x = 0.22	3.885	4.092	75.73 nm	9.15E-4	9.84E-5	1.05
x = 0.25	3.896	4.119	42.38	8.17E-4	5.56 E-5	1.05

### Microstructural or Morphological analysis

Microstructural as well as extent of porosity of prepared ferroelectric perovskites has been studied from microstructures recorded using scanning electron microscope. SEM micrographs of  $\text{Pb}_{1-x}\text{Gd}_x\text{TiO}_3$ , x = 0.22 & 0.25 ferroelectric perovskites solid solutions shown in figure 2. Squared shaped grains with cross linking reveals densification in prepared solid solutions. No free voids in microstructure reveals least porosity with maximum densifications. The microstructure clearly reveals that as concentration of  $\text{Gd}^{3+}$  increases at A-site in  $\text{PbTiO}_3$ , a gradual increase in grain size from x = 0.22 to 0.25 with simultaneous decrease in porosity due to increase in size of rare earth ion ( $\text{Gd}^{3+}$ ).

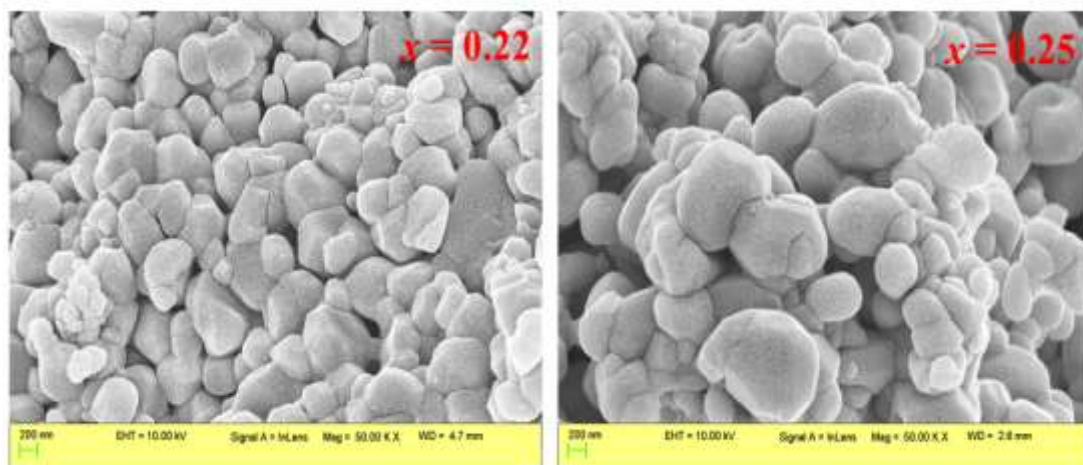


**Figure 2: SEM Micrographs of  $\text{Pb}_{1-x}\text{Gd}_x\text{TiO}_3$ , x = 0.22 & 0.25 ferroelectric perovskites solid solutions**

### Ferroelectric Properties

Shape of Polarization vs. Electric field curves gives information about presence or absence of ferroelectric polarization in prepared solid solutions. S-shaped saturated stamped for presence of ferroelectric properties in prepared solid solutions. Polarization vs. Electric field curves for  $\text{Pb}_{1-x}\text{Gd}_x\text{TiO}_3$ , x = 0.22 & 0.25 ferroelectric perovskites solid solutions have been shown in figure 3. It has been clearly seen from ferroelectric hysteresis curve that prepared ferroelectric perovskites exhibited Ferroelectric polarization which may appear due to the hybridization between 3d and 2p states of titanium and oxygen ions, respectively [40]. The remnant polarization ( $P_r$ ) for samples x = 0.22 and x = 0.25 is 20.83 and 10.93  $\mu\text{C}/\text{cm}^2$ , respectively. The

non-saturated S-shaped curve for sample  $x = 0.25$  also stamped for appearance of lossy behavior attributed due to increase in conductivity of sample resulted from oxygen vacancies led by hetro-valance substitution at  $\text{Pb}^{2+}$ . It has been clear from ferroelectric loops that as  $\text{Gd}^{3+}$  concentration increases at A-site in  $\text{PbTiO}_3$ , remnant polarizationdecreases/increases may be due to decrease in tetragonality or lattice distortion ( $c/a$  ratio) due to substitution of  $\text{Gd}^{3+}$  at  $\text{Pb}^{2+}$  site due to difference in atomic radii which also decreases unit cell volume. Decrease in lattice distortion has also be confirmed from decrease in value of maxima appears in  $\epsilon'$  vs. Temperature (K) profile. [18]. The remanent polarization ( $P_r$ ), saturation polarization ( $P_s$ ) and spontaneous polarization ( $P_{\text{spontaneous}}$ ) are given in table 2.

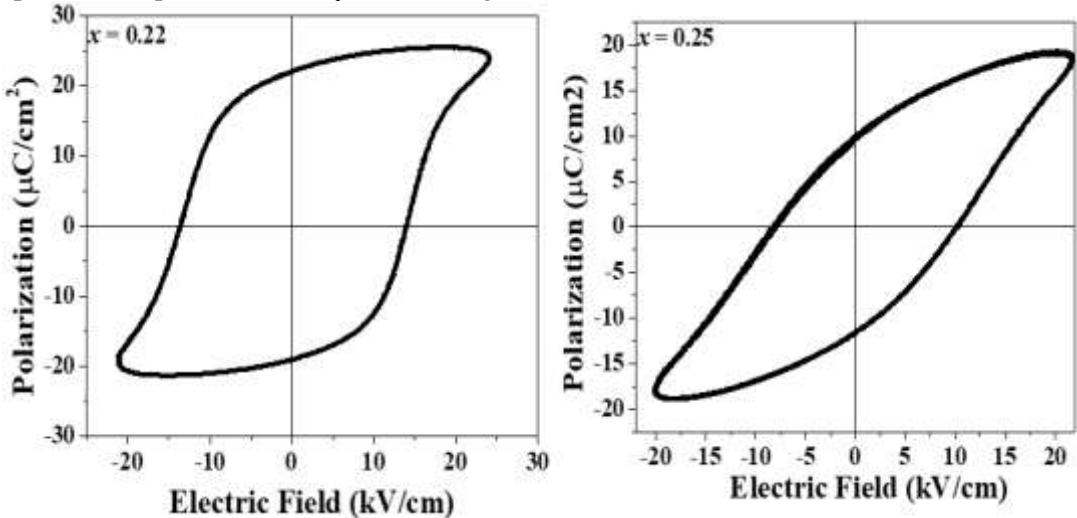


**Figure 3: ferroelectric Hysteresis Curve (Polarization vs. Applied Electric Field) of  $\text{Pb}_{1-x}\text{Gd}_x\text{TiO}_3$ ,  $x = 0.22$  &  $0.25$  ferroelectric perovskites**

**Table 2: The Remanent Polarization ( $P_r$ ), Saturation Polarization ( $P_s$ ) and Spontaneous Polarization ( $P_{\text{spontaneous}}$ ), Coercive Field (kV/cm) of  $\text{Pb}_{1-x}\text{Gd}_x\text{TiO}_3$ ,  $x = 0.22$  &  $0.25$  ferroelectric perovskites**

Sample Name	$P_r$ ( $\mu\text{C}/\text{cm}^2$ )	$P_s$ ( $\mu\text{C}/\text{cm}^2$ )	$P_{\text{spontaneous}}$ ( $\mu\text{C}/\text{cm}^2$ )	Coercive Field (kV/cm)
S1	20.83	25.72	11.33	13.33
S2	10.78	-----	2.45	9.02

### Ferroelectric Transition analysis

Influence of substitution of  $\text{Gd}^{3+}$  at  $\text{Pb}^{2+}$  site in  $\text{PbTiO}_3$  has also been analyzed from  $\epsilon'$  vs. Temperature (K) profile. Plot of  $\epsilon'$  vs. Temperature (K) profile (at different frequencies) of  $\text{Pb}_{1-x}\text{Gd}_x\text{TiO}_3$ ,  $x = 0.22$  &  $0.25$  ferroelectric perovskites solid solutionsshown in figure 4. It has been clearly visualized from graph that dielectric constant increases continuouslyachievea maximum upto certain limited value of temperature before it starts diminishes as temperature further increased implying a transition from ferroelectric to paraelectric phase. The ferroelectric transition temperature  $T_c^{\text{FE}}$  is  $\sim 603\text{K}$  &  $611\text{K}$  which is less than  $T_c^{\text{FE}}$  of  $\text{PbTiO}_3$

( $T_C^{FE} = 767\text{K}$ ). The lowered c/a ratio as compared to that of  $\text{PbTiO}_3$  [18] results in lowering lattice distortion leads to a decreased value of  $T_C^{FE}$ .

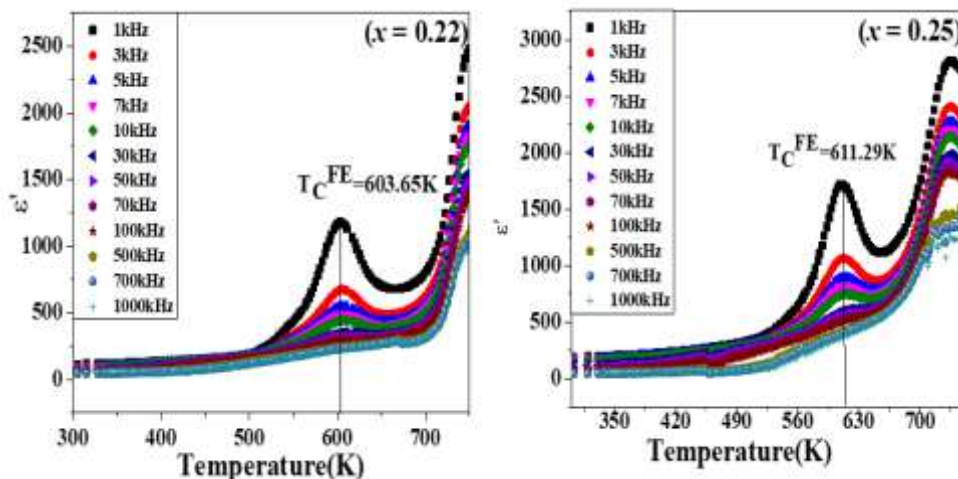


**Figure 4: Ferroelectric Transition Temperature Profile ( $\epsilon'$  vs. Temperature) of  $\text{Pb}_{1-x}\text{Gd}_x\text{TiO}_3$ ,  $x = 0.22$  &  $0.25$  ferroelectric perovskites**

Further  $\tan \delta$  vs. Temperature profile at different frequencies has also been recorded to analyze the presence of effect of temperature on dielectric relaxation.  $\tan \delta$  vs. Temperature profile of  $\text{Pb}_{1-x}\text{Gd}_x\text{TiO}_3$ ,  $x = 0.22$  &  $0.25$  ferroelectric perovskites has been shown in figure 5. It has been clearly seen in graphs that maxima in  $\tan \delta$  continuously shifted towards higher temperature regime at all recorded frequency evidence for presence of temperature dependent dielectric relaxation. To further confirm,  $Z''$  &  $M''$  vs. Frequency in full frequency range varied from  $0.1\text{ kHz}$  to  $1\text{ MHz}$  at different temperature have also been recorded and shown below.

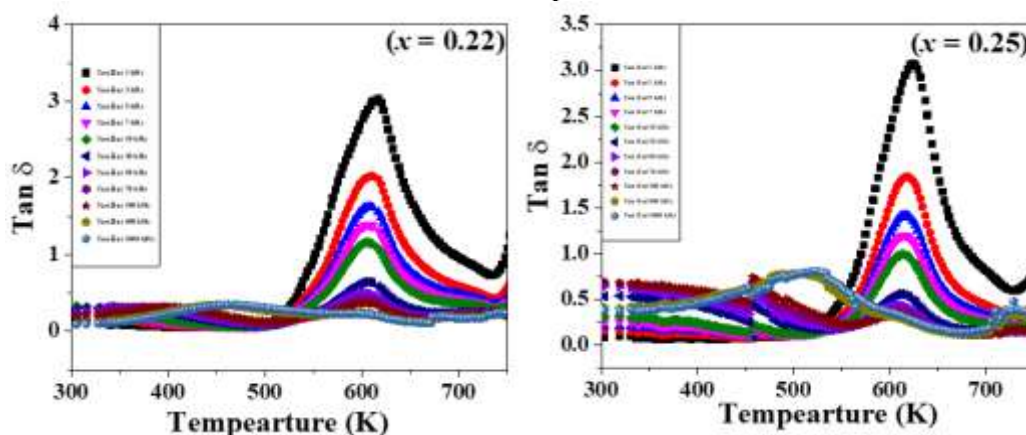


**Figure 5:  $\tan \delta$  vs. Temperature profile of  $\text{Pb}_{1-x}\text{Gd}_x\text{TiO}_3$ ,  $x = 0.22$  &  $0.25$  ferroelectric perovskites**

$Z''$  vs. Frequency (Hz) varied from 0.1 kHz to 1 MHz in temperature range 298K -773K of  $\text{Pb}_{1-x}\text{Gd}_x\text{TiO}_3$ ,  $x = 0.22$  & 0.25 ferroelectric perovskites have been shown in figure 6. The graphs clearly delineated that  $Z''$  increases first continuously with increasing frequency upto certain value and then starts decreases with further increase of frequency clearly overtaken the presence dielectric relaxations. The absence of maxima of  $Z''$  vs. Frequency directly evident for not presence of temperature dependent dielectric relaxation [19-21] and merging at higher temperatures reveals for elimination of space charge polarization.

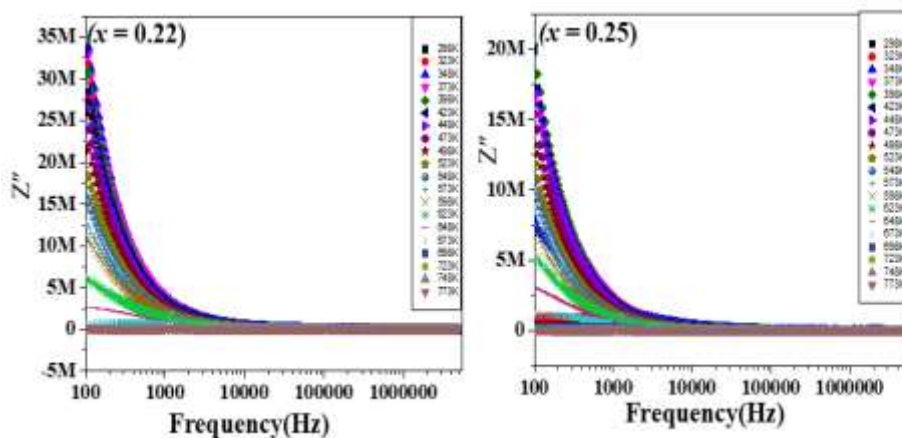


**Figure 6:**  $Z''$  vs. Frequency at Different Temperature profile of  $\text{Pb}_{1-x}\text{Gd}_x\text{TiO}_3$ ,  $x = 0.22$  & 0.25 ferroelectric perovskites

Dielectric Relaxation has also been analyzed from frequency dependence plots of  $M''$  at different temperature. Figure 7 display  $M''$  vs. Frequency (Hz) profile within frequency range varied from 0.1 kHz to 1 MHz in temperature range 298K -773K of  $\text{Pb}_{1-x}\text{Gd}_x\text{TiO}_3$ ,  $x = 0.22$  & 0.25 ferroelectric perovskites. Imaginary part of electrical modulus has been calculated from  $Z$  and phase angle ( $\theta$ ) using formula given below

$$M'' = \omega C_0 Z'$$

Where  $Z'$  is real part of impedance. It has been clearly depicted from graph that as frequency increases towards its high regime along with continuous increment in temperature, position of maxima (resonance frequency) in  $M''$  vs. frequency profiles ( $M''_{\max}$ ) has been continuously shifted towards high frequency region gives direct evidence for presence of temperature dependent hopping mechanism in electrical conduction. The non-Debye nature of dielectric relaxation with different time constant for relaxation response resulted from asymmetric broadening of the peak [22, 25]. The maxima of  $M''$  vs. frequency profiles ( $M''_{\max}$ ) in lower frequency regions claims of long range mobility of the ions whereas maxima of  $M''$  vs. frequency profiles ( $M''_{\max}$ ) peaks in high frequency regime reveals confinement of ions in potential wells within shorter distances range.

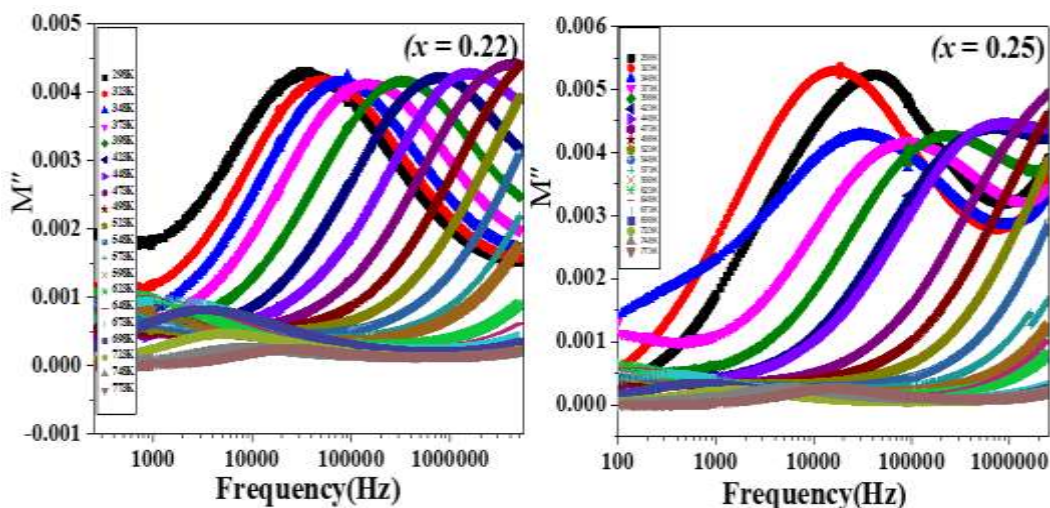


**Figure 7:  $M''$  vs. Frequency at Different Temperature profile of  $\text{Pb}_{1-x}\text{Gd}_x\text{TiO}_3$ ,  $x = 0.22$  &  $0.25$  ferroelectric perovskites**

#### Temperature Dependent Imaginary part of dielectric permittivity $\epsilon''$ vs. frequency analysis

Temperature dependent  $\epsilon'$  vs. Frequency varied from 0.1 kHz to 1 MHz in temperature range 298K - 773K of  $\text{Pb}_{1-x}\text{Gd}_x\text{TiO}_3$ ,  $x = 0.22$  &  $0.25$  ferroelectric perovskites has been shown in figure 8. The graphs clearly pictured out that both real and imaginary part of dielectric permittivity exhibits maximum value before 1kHz (means lower frequency regime) in certain frequency regime and later starts decreases continuously decreases with increasing frequency as well as temperature reveals dielectric behavior similar to normal dielectrics or standard dielectric response confirmed in prepared samples. The dielectric constant achieves two segments; one is maximum value (Real and Imaginary part of dielectrics) and other in which least value or almost shows frequency independence. The maximum value results due to existence of all polarizations (Ionic, Dipolar, Electronic & Space Charge Polarization) which contributes in dielectric constant and other in which continuous decrease of dielectric constant followed by linear independent variation of frequency may results due to elimination some polarizations (space charge polarization) at higher frequency regime. The graphs clearly appear as value of dielectric permittivity ( $\epsilon'$ ) first increases upto certain value of temperature and then decreases. It has also seen from graphs that dielectric constant increases with increasing temperature continuously upto certain value and then starts decreases reveals dielectric transition. Such type of response can be stated as that first increase may result due to easy orientation of dipoles w.r.t. to applied field due amount of sufficient energy received by dipoles to get easily orientates or sufficient energy to overcome thermal barrier energy comes from external heat. Apart from this range of temperature, dipole unable to responds properly results in temperature dependent dielectric relaxation. To further study in detail that either it may be Debye or non-Debye relaxation, experimental data has been fitted with theoretical model of Debye and non-Debye reported. [18-19]. Graphs have made it evident that the imaginary

component of the dielectric constant ( $\epsilon'$ ) first rises to a certain temperature before falling as the temperature rises further, indicating a temperature-dependent dielectric transition. Theoretically, this tendency can be described by the simultaneous increase in temperature and the dielectric constant, which may lead to easy dipole orientation with regard to the applied field. Additionally, temperature that transfers sufficient energy facilitates easy dipole orientation. These were sufficiently heated by outside sources or sufficiently heated to break through thermal barriers. Dielectric relaxation that is temperature-dependent happens when a dipole cannot react correctly outside of this temperature range.

The decrease in value of real dielectric permittivity with first increases upto certain value of Temperature and then starts decreases. Such type of behavior may be explained on basis of thermal energy provided to dipoles from heating. Due to this, response of dipoles towards applied field become easy results in increased in dielectric permittivity (Real part). Further increase of temperature made dipoles so relaxed that they unable to responds to applied signal results in further decreased in value of dielectric permittivity (Real part).

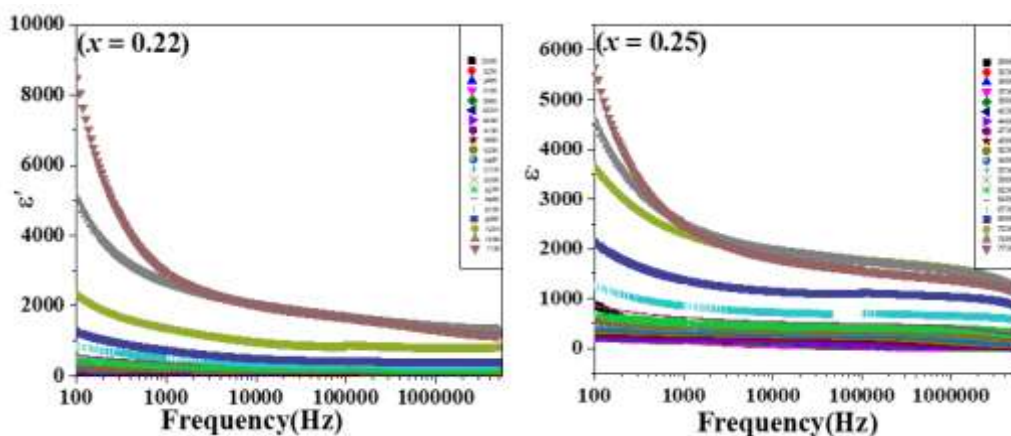


**Figure 8:**  $\epsilon'$  vs. Frequency at Different Temperature profile of  $\text{Pb}_{1-x}\text{Gd}_x\text{TiO}_3$ ,  $x = 0.22$  &  $0.25$  ferroelectric perovskites

### Temperature Dependent Imaginary part of dielectric permittivity $\epsilon''$ vs. frequency analysis

The change of  $\text{Pb}^{2+}$  with  $\text{Gd}^{3+}$  causes rise in concentration oxygen vacancies influences dielectric characteristics has also been investigated from temperature dependent dielectric properties of prepared ferroelectric solid solutions from imaginary part of dielectric constant ( $\epsilon''$ ) vs. Frequency profile at some selected temperatures. Temperature dependent  $\epsilon''$  vs. Frequency varied from 0.1 kHz to 1 MHz in temperature range 298K - 773K of  $\text{Pb}_{1-x}\text{Gd}_x\text{TiO}_3$ ,  $x = 0.22$  &  $0.25$  ferroelectric perovskites has been shown in figure 9. Dielectric transition response has also been studied from such type of behavior in which prepared sample reveals from decreasing response from initially increasing response in value of dielectric constant ( $\epsilon'$ ) vs. with increasing temperature beyond a certain fixed value. Decreasing from maximum value of dielectric constant ( $\epsilon''$ ) with continuous increasing frequency signature for presence of behavior of normal dielectrics or Debye behavior in prepared ferroelectric solid solutions. A

prepared sample shows a diminishing reaction from an originally growing response in the dielectric constant ( $\epsilon''$ ) value vs. with increasing temperature beyond a particular fixed value. This type of behavior has also been used to study the dielectric transition response. In prepared ferroelectric solid solutions, the dielectric constant ( $\epsilon''$ ) decreases from its maximum value while the frequency signature continuously increases to indicate the presence of normal dielectric or Debye behavior. Figure 9 displays the temperature-dependent imaginary portion of the dielectric constant ( $\epsilon''$  vs. frequency (Hz)) of ferroelectric solid solutions of  $\text{Gd}_x\text{Pb}_{1-x}\text{TiO}_3$ , where  $x = 0.22$  &  $0.24$ , in the temperature range of 298K-773K. The imaginary portion of the dielectric constant ( $\epsilon''$ ) reaches its maximum value in the lower frequency range and steadily decreases as the frequency rises. The imaginary portion of the dielectric constant ( $\epsilon''$ ) becomes constant and independent of frequency after a certain value. In prepared ferroelectric solid solutions, this kind of response validates typical dielectric behavior. All polarizations (ionic, dipolar, electronic, and space charge polarization) contributed differently with different frequency ranges, which is why the imaginary component of the dielectric constant ( $\epsilon''$ ) varied with frequency. Graphs have made it evident that the imaginary component of the dielectric constant ( $\epsilon''$ ) first rises to a certain temperature before falling as the temperature rises further, indicating a temperature-dependent dielectric transition. Theoretically, this tendency can be described by the simultaneous increase in temperature and the dielectric constant, which may lead to easy dipole orientation with regard to the applied field. Additionally, temperature that transfers sufficient energy facilitates easy dipole orientation. These were sufficiently heated by outside sources or sufficiently heated to break through thermal barriers. Dielectric relaxation that is temperature-dependent happens when a dipole cannot react correctly outside of this temperature range.[21-22]. The thermal energy that heating gives dipoles explains this type of behavior. Consequently, dipoles respond more readily to applied fields, increasing their dielectric permittivity (Imaginary portion). The dielectric constant rises as the temperature rises because of the increased mobility of charge carriers. This effect is caused by interfacial polarization rather than dipolar polarization. The primary reason why dispersion loss rises with temperature and frequency is thermal vibrations. The value of  $\epsilon'$  is no longer affected by interfacial polarization.

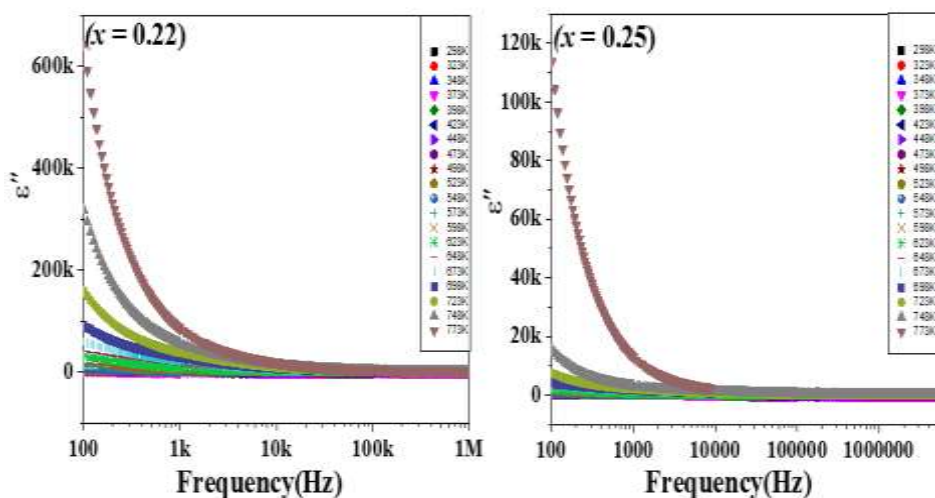


**Figure 9:  $\square'$  vs. Frequency at Different Temperature profile of  $\text{Pb}_{1-x}\text{Gd}_x\text{TiO}_3$ ,  $x = 0.22$  &  $0.25$  ferroelectric perovskites**

$Z'$  vs. Frequency varied from 0.1 kHz to 1 MHz in temperature range 298K -773K of  $\text{Pb}_{1-x}\text{Gd}_x\text{TiO}_3$ ,  $x = 0.22$  &  $0.25$  ferroelectric perovskites have been shown in figure 10. The graphs clearly delineated that as frequency and temperature increases simultaneously,  $Z'$  decreases manifest that prepared samples exhibit negative temperature coefficient of resistance (NTCR) [22]. The decrease in value of  $Z'$  with increasing temperature directly proclaim the reduction in resistive properties followed by increasing conductive behavior due to increasing concentration of  $\text{Gd}^{3+}$  in prepared ceramic ferroelectric solid solutions. The decreased resistive behavior or barrier can also be justified from temperature dependent conductivity profile. The increase in conductivity with temperature may results due to increase in concentration of oxygen vacancies with increasing temperature. [24-26]. The inverse relationship between temperature and  $Z'$  indicates that as ferrite concentration increases in prepared ceramic composites, resistive qualities drop and conductive behavior increases. The temperature-dependent conductivity profile also provides justification for the reduced resistive behavior or barrier. An increase in concentration may be the cause of the conductivity's temperature increase. The increase in conductivity with temperature may results due to increase in concentration of oxygen vacancies with increasing temperature.

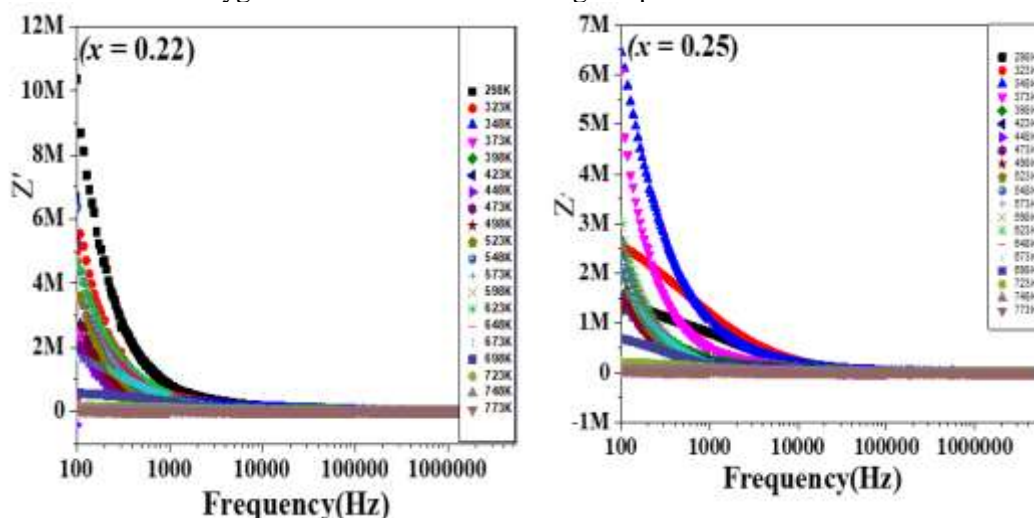


**Figure 10:  $\square'\square'$  vs. Frequency at Different Temperature profile of  $\text{Pb}_{1-x}\text{Gd}_x\text{TiO}_3$ ,  $x = 0.22$  &  $0.25$  ferroelectric perovskites**

$M'$  vs. Frequency varied from 0.1 kHz to 1 MHz in temperature range 298K -773K of  $\text{Pb}_{1-x}\text{Gd}_x\text{TiO}_3$ ,  $x = 0.22$  &  $0.25$  ferroelectric perovskites have been shown in figure 11. The graphs clearly delineated that as frequency and temperature increases simultaneously,  $M'$  decreases manifest that prepared samples exhibit negative temperature coefficient of resistance (NTCR) [22]. The decrease in value of  $M'$  with increasing temperature directly stamped decreases in insulating behavior led by increasing conductive behavior due to increasing concentration of  $\text{Gd}^{3+}$  in prepared ceramic ferroelectric solid solutions. The substitution of  $\text{Gd}^{3+}$  results in

increase in concentration of oxygen vacancies due to charge im-balance created by  $Gd^{3+}$  substitution at  $Pb^{2+}$  in  $PbTiO_3$  ferroelectric ceramic solid solutions. The decreased resistive behavior or barrier can also be justified from temperature dependent conductivity profile. The increase in conductivity with temperature may results due to increase in concentration of oxygen vacancies with increasing temperature. [24-26]. The inverse relationship between temperature and  $M'$  indicates that as ferrite concentration increases in prepared ceramic composites, resistive qualities drop and conductive behavior increases. The temperature-dependent conductivity profile also provides justification for the reduced resistive behavior or barrier. An increase in concentration may be the cause of the conductivity's temperature increase. The increase in conductivity with temperature may results due to increase in concentration of oxygen vacancies with increasing temperature.

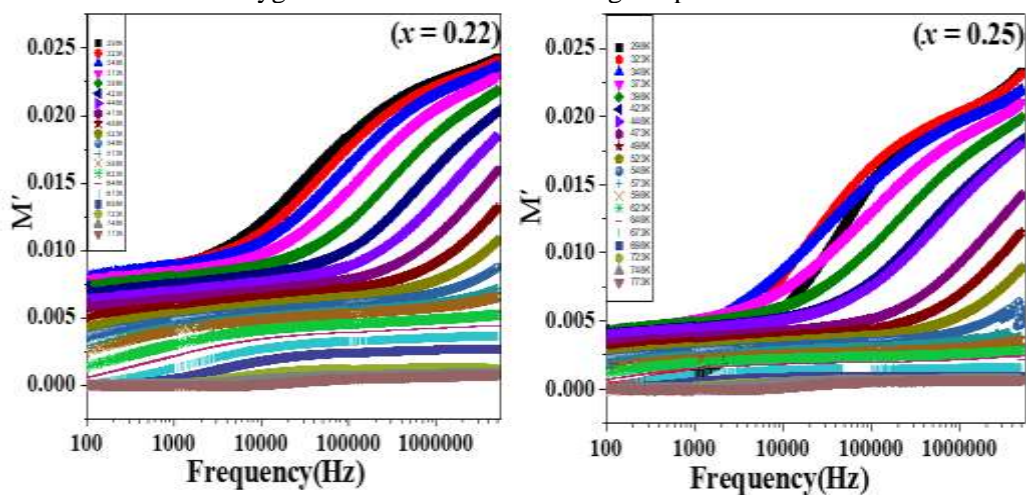


**Figure 11:**  $M''$  vs. Frequency at Different Temperature profile of  $Pb_{1-x}Gd_xTiO_3$ ,  $x = 0.22$  &  $0.25$  ferroelectric perovskites

figure 12 shows the frequency dependence of electrical conductivity for  $Pb_{1-x}Gd_xTiO_3$ ,  $x = 0.22$  &  $0.25$  ferroelectric perovskites ferroelectric ceramics at room temperature. The ac conductivity is calculated from the measured dielectric data using the relation:

$$\sigma_{ac} = 2\pi f \epsilon' \epsilon_0 \tan \delta [18],$$

where the parameters have their usual meaning. It can be observed that the ac conductivity increases with increasing frequency for all compositions. It is further clear from the figure that the conductivity shows two distinct regimes within the measured frequency limit, (i) the plateau and (ii) the dispersion region. The plateau region corresponds to low frequency region. In this region, the conductivity has been found to be independent of frequency. The dispersion region corresponds to high frequency region. In this region, conductivity increases with increase in frequency. In fact, the plateau region corresponds to dc conductivity ( $\sigma_{dc}$ ) and dispersion region corresponds to ac conductivity ( $\sigma_{ac}$ ). The frequency dependence of ac conductivity in ceramics is generally analyzed by Jonscher's power law [18];

$$\sigma_{ac} = \sigma_{dc} + A \omega^n,$$

where “A” is the dispersion parameter representing the strength of polarizability and “n” is the dimensionless frequency exponent representing the interaction between mobile ions with the lattice around them [19].

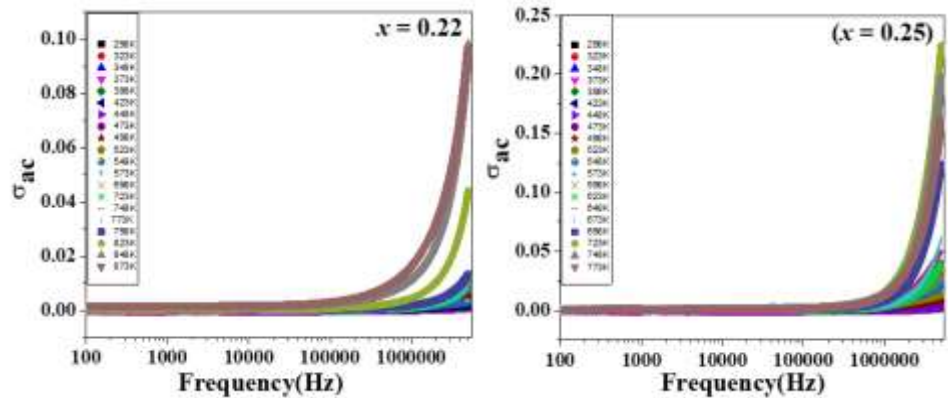


**Figure 11:**  $\sigma_{ac}$  vs. Frequency at Different Temperature profile of  $Pb_{1-x}Gd_xTiO_3$ ,  $x = 0.22$  &  $0.25$  ferroelectric perovskites

It has been clearly perceived from graphs that conductivity increases with increasing temperature. The increase of oxygen vacancies due to temperature may result in an uninterrupted increase in electrical conductivity [21-22].

The effect of oxygen vacancies created by  $Gd^{3+}$  substitution at  $Pb^{2+}$  in  $PbTiO_3$  ferroelectric ceramic solid solution results in charge imbalance which increases the concentration of oxygen vacancies in modified  $PbTiO_3$  ferroelectric ceramic solid solutions. The increase in conductivity with temperature has directly been emphasized from Figure 12. The increase in conductivity with temperature may result due to an increase in the concentration of oxygen vacancies with increasing temperature.

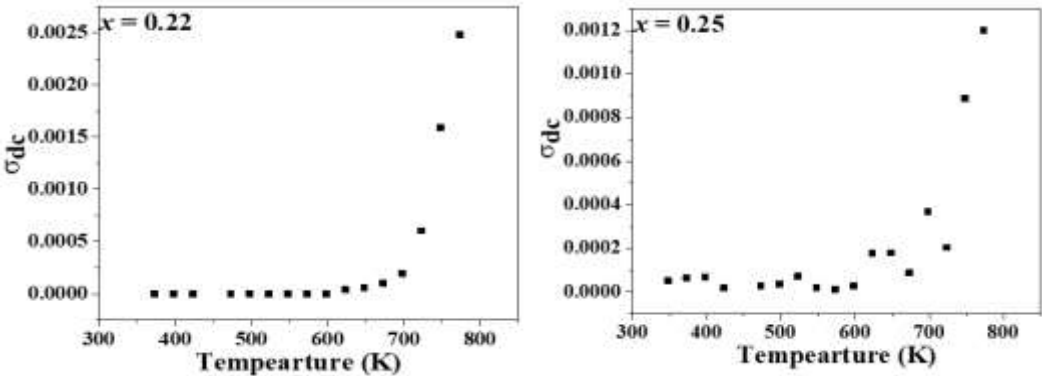


**Figure 12:** Variation of  $\sigma_{dc}$  (obtained from Jonscher ‘power law fitting’) of  $Pb_{1-x}Gd_xTiO_3$ ,  $x = 0.22$  &  $0.25$  ferroelectric perovskites for Conduction Mechanism

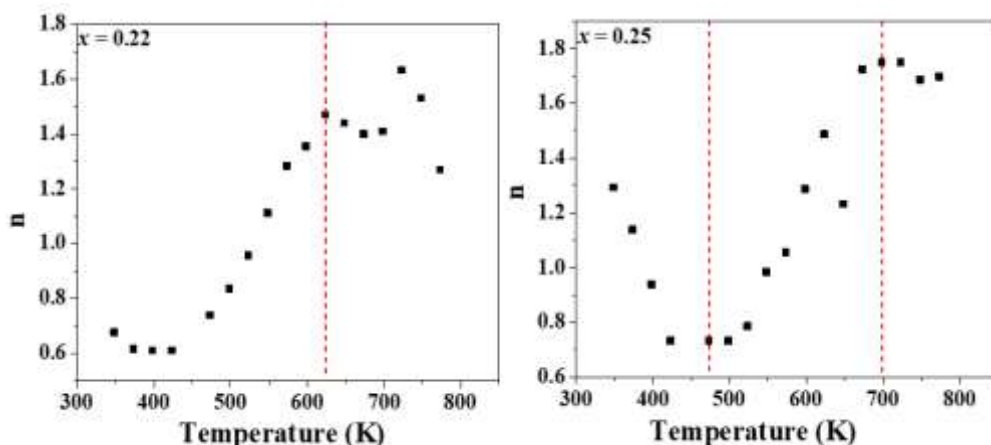


**Figure 13: Variation of  $n$  (obtained from Jonscher 'power law fitting') of  $\text{Pb}_{1-x}\text{Gd}_x\text{TiO}_3$ ,  $x = 0.22$  &  $0.25$  ferroelectric perovskites for Conduction Mechanism**

figure 13 shows the variation of  $n$  versus temperature for of  $\text{Pb}_{1-x}\text{Gd}_x\text{TiO}_3$ ,  $x = 0.22$  &  $0.25$  ferroelectric perovskites for Conduction Mechanism. According to CBH (Correlated Barrier Hopping Model),  $n$  decreases with increasing temperature whereas in OLPT (Overlapping Large Polaron Tunneling Model),  $n$  first decreases with increasing temperature upto certain lower value then increases with further increase in temperature. In QMT (Quantum mechanical Tunneling Model), the value of  $n \sim 0.8$  and is temperature independent [24-29]. From figure 13, sample  $x = 0.22$ ,  $n$  first decreases and then with increasing temperature upto  $630^\circ\text{C}$  and then starts increases with increasing of temperature reveals that prepared ferroelectric ceramic solid solutions exhibits Correlated Barrier Hopping Model whereas in sample  $x = 0.24$ ,  $n$  first decreases with increasing temperature upto  $480^\circ\text{C}$  and then increases with increasing in temperature upto to  $700^\circ\text{C}$  and then decreases. So sample exhibits Correlated Barrier Hopping Model in region I to II and Carrier Barrier Hopping –CBH or small polaron tunneling (NSPT) in region III.

Real part of Impedance( $Z'$ ) vs Imaginary Part of impedance ( $Z''$ ) analysis: Cole-Cole Plot

To study contribution of grain and grain boundaries in electrical properties of prepared ceramic composites,  $Z''(\Omega)$  vs.  $Z'(\Omega)$  profile in temperature range varies from 298K-773K of  $\text{Gd}_x\text{Pb}_{1-x}\text{TiO}_3$ ,  $x = 0.22$  &  $0.25$ ) ferroelectric solid solutions shown on figure 14. Cole-Cole plots which consists of semicircles provide details on various relaxation processes. These semicircles show relaxation caused by the grain boundary in lower frequency zone, while grains alone cause relaxation in the higher frequency region. Due to a variety of circumstances, such as grain orientation, grain boundaries, and the distribution of structural defects, the semicircles show some depression with their centers below the real axis, exhibiting non-Debye behavior [18-23].

Theoretically, fitted Nyquist plots have been studied using a suitable equivalent circuit of Resistance ( $R$ ) – Capacitance ( $C$ ) which explain contribution of grain and grain boundaries towards electrical properties. Such combination of Resistance ( $R$ ) – Capacitance ( $C$ ) in equivalent circuit depends upon number of semi circles appear in experimental data. A grain

circuit is represented by parallel combination of  $R_g$  and  $C_{PEg}$ , whereas for grain boundaries are represented by parallel combination of  $R_{gb}$  and  $C_{PEgb}$ . A constant phase element (CPE) signifies a departure from perfect Debye behavior.  $Z_{CPE} = 1/(j\omega)^\beta$  CPE, where  $\beta \leq 1$ . The equation for the equivalent circuit can be represented by  $Z^*(\omega) = Z' + jZ''$  where

$$Z' = \frac{R_g}{1 + (\omega_g R_g C_g)^2} + \frac{R_{gb}}{1 + (\omega_{gb} R_{gb} C_{gb})^2}$$

$$Z'' = \frac{\omega_g R_g^2 C_g}{1 + (\omega_g R_g C_g)^2} + \frac{\omega_{gb} R_{gb}^2 C_{gb}}{1 + (\omega_{gb} R_{gb} C_{gb})^2}$$

Resistance, capacitance, and frequency are represented at the peaks of semicircles for grain and grain boundary by ( $R_g$ ,  $C_g$ ,  $\omega_g$ ) & ( $R_{gb}$ ,  $C_{gb}$ ,  $\omega_{gb}$ ). It has been clearly visualized from graphs that in samples,  $x = 0.22$ , exhibits for appearing semicircle as temperature increases reveals contribution of grains only in dielectric and impedance properties whereas in sample  $x = 0.24$ , appearance of second semicircle manifest that in prepared ferroelectric ceramic solid solutions, grains and grain boundaries contributes in dielectric and impedance properties.

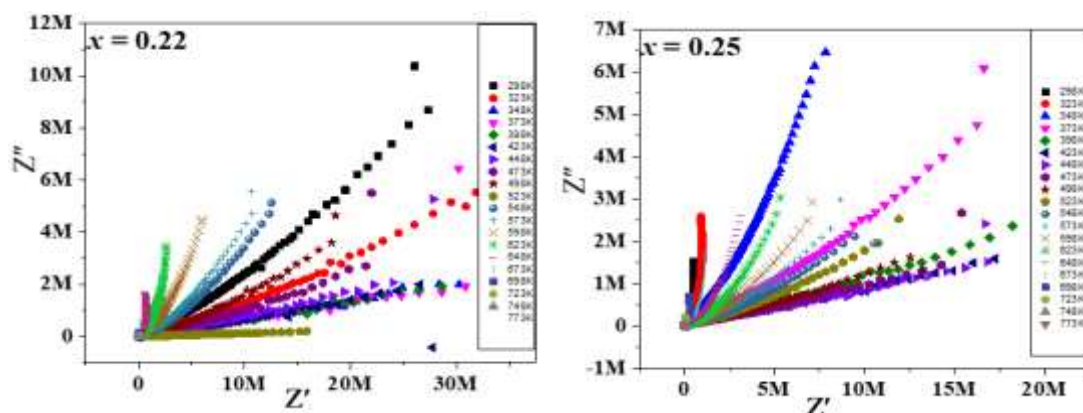


**Figure 14:**  $Z''$  vs.  $Z'$  at Different Temperature profile of  $Pb_{1-x}Gd_xTiO_3$ ,  $x = 0.22$  &  $0.25$  ferroelectric perovskites

The maxima in  $Z''$  vs. frequency shows appearance of resonance in prepared ceramic solid solutions. Figure 15 display  $Z'$  vs. Frequency (Hz) profile of  $Pb_{1-x}Gd_xTiO_3$ ,  $x = 0.22$  &  $0.25$  ferroelectric perovskites. Imaginary part of impedance has been calculated from real part of impedance using formula given below

$$Z'' = |Z| \sin(\theta)$$

It has been clearly seen from graphs that value of imaginary part of impedance ( $Z''$ ) first increases continuously with increasing frequency and achieved maximum value and then starts decreases with continuous increase in frequency. The maxima of  $Z''$  at particular frequency known as resonance frequency at which frequency of ion resonates with frequency of externally applied electric field clearly reveals presence dielectric relaxations. The continuous shift in maxima of  $Z''$  with Frequency as well as temperature evident for presence of frequency and temperature dependent dielectric relaxation. The disappearing of maxima in value of

imaginary part of impedance (merging at higher temperatures) reveals for elimination of space charge polarization [22-24].

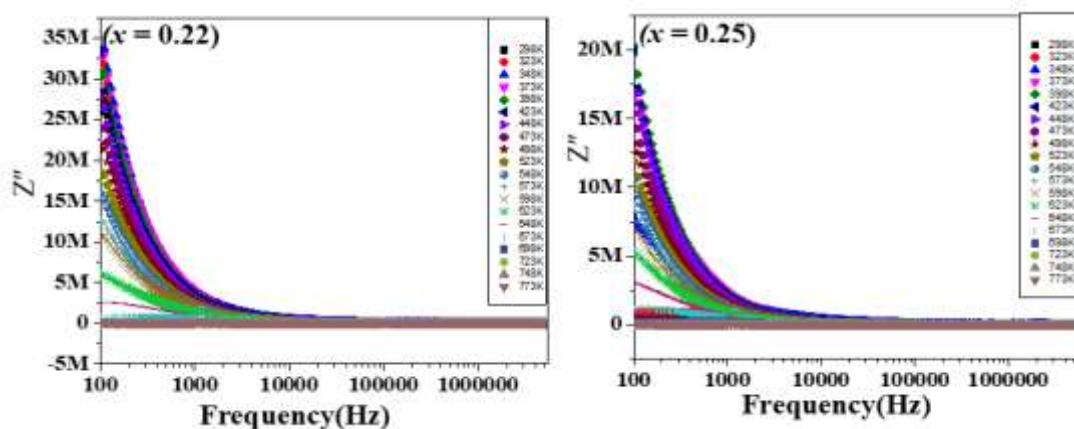


**Figure 15:**  $Z''$  vs. frequency (Hz) at Different Temperature profile of  $\text{Pb}_{1-x}\text{Gd}_x\text{TiO}_3$ ,  $x = 0.22$  &  $0.25$  ferroelectric perovskites

#### 4. Conclusion

Trivalent metal ion ( $\text{Gd}^{3+}$ ) modified  $\text{PbTiO}_3$  ( $\text{Pb}_{1-x}\text{Gd}_x\text{TiO}_3$ ,  $x = 0.22$  &  $0.25$ ) ferroelectric perovskites have been synthesized using solid solutions. Structural phase of crystallization of  $\text{Pb}_{1-x}\text{Pr}_x\text{TiO}_3$ ,  $x = 0.22$  &  $0.25$  has been confirmed from peak at  $2\theta \sim 32$  in X-ray diffraction data to analyze structural phase formed and average crystallite size calculated using Debye Scherer formula. Structural analysis reveals that prepared ferroelectric ceramic solid solutions exhibit single phase tetragonal crystal structure. Ferroelectric properties confirmed from S-shaped ferroelectric hysteresis recorded in form of Polarization vs. Electric Field curve and reveals that ferroelectric polarization decreases with increasing  $\text{Gd}^{3+}$  content which results in increased oxygen vacancies led increased conductive behavior. This decreased ferroelectric polarization has also been confirmed from decreased in tetragonality led by increasing  $\text{Gd}^{3+}$  content also stamped from decreased ferroelectric transition temperature confirmed from  $\epsilon'$  vs. Temperature Profile. Maxima in  $\epsilon'$  vs. Temperature profile represents transition from ferroelectric phase of modified  $\text{PbTiO}_3$  to paraelectric phase transition whereas lower  $T_c^{\text{FE}}$  corresponds to decreased in tetragonality due to partial substitution of  $\text{Gd}^{3+}$  at  $\text{Pb}^{2+}$  which may be signature of shifts of non-centrosymmetry of unit cell to centrosymmetric unit.  $Z'$  as well as  $M'$  decreases with increase in temperature and frequency, suggesting that materials exhibit negative temperature coefficient of resistance (NTCR). Such decrease in value of  $Z'$  reveals deterioration in resistive behavior of prepared ferroelectric ceramic perovskites. The dielectric relaxation appears as substitution of  $\text{Pr}^{3+}$  increases and continuously shifts towards maximum frequency regime which reveals disappearing of dielectric relaxation. The semicircle in Nyquist plots reveals contribution of grain and grain boundaries in electrical properties. The effect of valancydiffere in parent and substituted ion leads in creation of oxygen vacancies responsible for improvement in conductivity has been analyzed and reported. sample  $x = 0.22$ ,  $n$  first decreases and then with increasing temperature upto  $630^\circ\text{C}$  and then starts increases

with increasing of temperature reveals that prepared ferroelectric ceramic solid solutions exhibits Correlated Barrier Hopping Model whereas in sample  $x = 0.24$ ,  $n$  first decreases with increasing temperature upto 480 °C and then increases with increasing in temperature upto to 700 °C and then decreases. So sample exhibits Correlated Barrier Hopping Model in region I to II and Carrier Barrier Hopping –CBH or small polaron tunneling (NSPT) in region III.

## References:

1. L. Chen, T.W. Li, S. Cao, S. Yuan, F. Hong and J.C. Zhang, The role of 4f-electron on spin reorientation transition of NdFeO<sub>3</sub>: A first principle study, *J. Appl. Phys.* 111, 103905 (2012).
2. S. Yuan, Y. Wang, M. Shao, F. Cheng, B. Kang and Y. Isikawa, Magnetic properties of NdFeO<sub>3</sub> single crystal in spin reorientation region, *J. Appl. Phys.* 109, 07E144 (2011).
3. P.V. Serna, C.G. Campos, F. Sanchez, D. Jesus, A.M.B. Miro, J. Antonics, J. Coran and J. Longwell, Mechano-synthesis, crystal structure and magnetic characterization of Neodymium ferrite, *Material Research*, 19 (2), 389-393 (2016).
4. S.A. Mir, M. Ikram and K. Asokan, Structural, optical and dielectric properties of Ni substituted NdFeO<sub>3</sub>, *Optik* 125, 6903-6908 (2014).
5. A. Bashir, M. Ikram, Ravi Kumar, P. Thakur, K.H. Chae, W.K. Choi and V.R. Reddy, Structural, magnetic and electronic structure studies of NdFe<sub>1-x</sub>Ni<sub>x</sub>O<sub>3</sub> (0 ≤  $x$  ≤ 0.3), *J. Phys.: Condens. Mater* 21, 325501 (2009).
6. I. Ahmad, M.J. Akhtar, M. Younas, M. Siddique and M.M. Hasan, Small Polaronic hole hopping mechanism and Maxwell Wanger relaxation in NdFeO<sub>3</sub>, *J. Appl. Phys.* 112, 074105 (2012).
7. W. Slawinski, R. Prezenioslo and I. Sosowska, Spin reorientation and structural changes in NdFeO<sub>3</sub>, *J. Phys.: Condens. Mater* 17, 4605-4614 (2005).
8. G.R. Hearne, M.P. Pasternak, R.D. Taylor and P. Lacorre, Electronic structure and magnetic properties of LaFeO<sub>3</sub> at high pressure, *Physical Review B* Vol. 51 No. 17 (1995).
9. G. Gorodetsky, B. Sharon and S. Shtrikman, Magnetic properties of an Antiferromagnetic Orthoferrites, *J. Appl. Phys.* 39 No. 2 (1968).
10. S. Chanda, S. Saha, A. Dutta and T.P. Sinha, Raman spectroscopy and dielectric properties of nanoceramic NdFeO<sub>3</sub>, *Material Research Bulletin*, 48, 1688-1693 (2013).
11. V.A. Chaudhari and G.K. Bichile, Synthesis, Structural, and Electric Properties of Pure PbTiO<sub>3</sub> Ferroelectric ceramics, *Smart Materials research 2013* (2013) Article ID 147524.
12. M. Mir, C.Cd. Paula, D. Garcia, R.H.G.A. Kiminami, J.A. Eiras, Y.P. Mascarenhas, Microstructural characterization using the RIETVELD Method in lead lanthanum titanate ceramics system produced by combustion synthesis, *Journal of European Ceramic Society.* 27 (2007) 3719-3721.
13. Khomskii DI (2006) Multiferroics: Different ways to combine magnetism and ferroelectricity. *J Magn Magn Mater* 306:1–8. <https://doi.org/10.1016/j.jmmm.2006.01.238>
14. F. Huang, X. Lu, W. Lin, X. Wu, Y. Kan and J. Zhu, Effect of Nd dopant on magnetic and electric properties of BiFeO<sub>3</sub> thin films prepared by metal organic deposition method, *Appl. Phys. Lett.* 89 (2006) 242914-3.
15. G.D. Hu, X. Cheng, W.B. Wu and C.H. Yang, Effects of Gd substitution on structure and ferroelectric properties of BiFeO<sub>3</sub> thin films prepared using metal organic decomposition, *Appl. Phys. Lett.* 91 (2007) 232909-3.
16. Tiku Ram, Akshay, Kanchan Khanna, Sunil K. Dwivedi and Sunil Kumar, Effect of Synthesis method on Structural, Ferroelectric and conduction relaxation in Pb<sub>1-x</sub>La<sub>x</sub>TiO<sub>3</sub>, where  $x = 0.25$  ceramics, *Material Today Proceedings*, Vol. 65 Part 1 (2022) 327-331, doi:10.1016/j.matpr.2022.06.206

17. Correlation between Sintering Temperature and Structural, Ferroelectric Properties of  $\text{Pb}_{0.75}\text{Nd}_{0.25}\text{TiO}_3$  Ceramics, Akshay Kumar, Tiku Ram, Kanchan Khanna, Sunil K. Dwivedi and Sunil Kumar, *Material Today Proceedings*, Vol. No. 65 Part 1(2022) 322-326
18. M. Kumar, K. L. Yadav, *J. Phys.: Condens. Matter*, 19 (2002) 242202.
19. K. S. Cole, H. Robert, "Dispersion and Absorption in Dielectrics:- Alternating Current Characteristics". *Journal of Chemical Physics*, 9 (1941) 341–351.
20. S. Havriliak, S. Negami, A complex plane representation of dielectric and mechanical relaxation processes in some polymers. *Polymer* 8: 161-210. DOI: 10.1016/0032-3861 (1967) 90021-3.
21. V. Prakash, S. N. Choudhary, T. P. Sinha, "Dielectric relaxation in complex perovskite oxide  $\text{BaCo}_{1/2}\text{W}_{1/2}\text{O}_3$ " *Physica B*, vol.403, pp.103–108, 2008.
22. A. K. Jonscher, *Nature* 267, 673 (1977).
23. D. K. Pradhan, B. Behera, P. R. Das, *J. Mater. Sci. Mater. Electron*, 23 (2012) 779.
24. J.C. Dyre, Th.B. Schroder, "Ac hopping conduction at extreme disorder takes place on the percolating cluster", *Phys. Stat. Sol. B*, vol. 230 (2002) pp.5.
25. M. Shariq, D. Kaur, V.S. Chandel, M.A. Siddiquia, *Acta Physica Polonica A*, Vol. 127 (2015) 1675-1679.
26. S. Pattanayak, R. N. P. Choudhary, P. R. Das, *J. Mater. Sci. Mater. Electron*, 24 (2013) 2667-2771.
27. G. Catalan, J. F. Scott, *Adv. Mater.* 21 (2009) 2463.
28. M. Tan, V. Koseoglu, F. Alan and E. Senturk, Overlapping large Polaron tunneling conductivity and giant dielectric constant in  $\text{Ni}_{0.5}\text{Zn}_{0.5}\text{Fe}_{1.5}\text{Cr}_{0.5}\text{O}_4$  nanoparticles (NPs), *Journal of Alloys and Compounds*, 509 (2011) 9399-9405.
29. R. Vaish and K.B.R. Varma, Dielectric properties of  $\text{Li}_2\text{O}-3\text{B}_2\text{O}_3$  glasses, *J. Appl. Phys.* 103, (2009) 064106.
30. M. Megdiche, C.P. Pellegrino and M. Gargouri, Conduction mechanism study by overlapping large Polaron tunneling model in  $\text{SrNiP}_2\text{O}_7$  ceramic compound, *Journal of Alloys and Compounds*, 584 (2014) 209-215.